Appl Microbiol Biotechnol (2005) 69: 326–334
DOI 10.1007/s00253-005-1988-0

Hong Yin · Thomas K. Wood · Barth F. Smets

Reductive transformation of TNT by *Escherichia coli* resting cells: kinetic analysis

Received: 14 December 2004 / Revised: 23 March 2005 / Accepted: 31 March 2005 / Published online: 19 April 2005

Abstract Microbial 2,4,6-trinitrotoluene (TNT) biotransformation via sequential nitro-reduction appears a ubiquitous process, but the kinetics of these transformations have been poorly understood or described. TNT transformation by *Escherichia coli* was monitored and a kinetic model for reductive TNT depletion was developed and experimentally calibrated in this report. Using resting cells of aerobically pregrown *E. coli*, TNT was quickly reduced to hydroxylaminodinitrotoluenes. The standard Michaelis–Menten model was modified to include three additional parameters: product toxicity (T_c), substrate inhibition (K_i), and intracellular reducing power (RH) limitation. Experimentally measured product toxicity (5.2 μmol TNT/mg cellular protein) closely matched the best-fit model value (2.84 μmol TNT/mg cellular protein). Parameter identifiability and reliability (k_m, K_s, T_c, and K_i) was evaluated and confirmed through sensitivity analyses and via Monte Carlo simulations. The resulting kinetic model adequately described TNT reduction kinetics by *E. coli* resting cells in the absence or presence of reducing power limitation.

H. Yin · B. F. Smets
Department of Civil and Environmental Engineering,
University of Connecticut,
Storrs, CT 06269, USA

T. K. Wood
Department of Chemical Engineering,
University of Connecticut,
Storrs, CT 06269, USA

T. K. Wood · B. F. Smets
Department of Molecular and Cell Biology,
University of Connecticut,
Storrs, CT 06269, USA

B. F. Smets (✉)
Environment and Resources DTU,
Technical University of Denmark,
Bldg 115,
2800 Kgs. Lyngby, Denmark
e-mail: bfs@er.dtu.dk
Tel.: +45-45-252230
Fax: +45-45-932850

Introduction

2,4,6-Trinitrotoluene (TNT) has been extensively produced for the generation of explosives, dyestuffs, and photographic chemicals (Sax and Lewis 1987). It has caused severe contamination of soil and water, and is mutagenic and potentially carcinogenic (Dodard et al. 2003; Honeycutt et al. 1996). Thus, remediation of TNT-contaminated environments is deemed necessary to protect human and ecosystem health.

The combined steric and electrophilic effects of multiple nitro substitutions on the aromatic nucleus make TNT apparently recalcitrant to oxygenolytic transformation (Esteve-Núñez et al. 2001; Preuss and Rieger 1995) and even aerobic bacteria tend to transform TNT by sequential reductive transformation of the nitro groups via hydroxylamino to the corresponding amines (Esteve-Núñez et al. 2001; McCormick et al. 1976). Reduction of TNT beyond diaminonitrotoluenes (DANT) is typically not observed (Esteve-Núñez et al. 2001; Fuller and Manning 1997; Labidi et al. 2001). Reductive transformation of TNT has been documented in many bacterial genera and by many enzymes, and is generally considered a cometabolic reaction (Fiorella and Spain 1997; Huang et al. 2000; Watrous et al. 2003), but reports on kinetic analysis of the observed TNT transformations have been sparse. Efforts to kinetically describe the fate of TNT during reductive cometabolic transformation in a fed-batch reactor yielded poor results (Daun et al. 1999a,b).

Although factors such as initial TNT concentration (Daun et al. 1999a,b; Fuller and Manning 1997; Gibbs et al. 2001), NAD(P)H concentration (Riefler and Smets 2002; van Beelen and Burris 1995; Zenno et al. 1996a,b, 1998), and exogenous electron donor availability (Adrian et al. 2003; Lewis et al. 1996; Park et al. 2002a,b) have all been reported to impact the rate and extent of TNT transformation, while toxicity after TNT exposure (Homma-Takeda et al. 2002; Kurinenko et al. 2003; Oh et al. 2003; Riefler and Smets 2002) has been noted, these observations have so far not been captured in a comprehensive kinetic model. On the other hand, cometabolic transformation of other organic chemicals has received substantial quantitative bio-

kinetic treatment (Criddle 1993), providing a rich resource of models.

The goal of this study was, therefore, to initiate development of a kinetic model to describe reductive TNT transformation by whole cell, and calibrate it in resting cells assays with an *Escherichia coli*-type strain.

Materials and methods

Chemicals TNT was purchased from Chemservice (West Chester, PA.). Analytical standards of TNT, 2-hydroxylamino-4,6-dinitrotoluene (2HA46DNT), 4-hydroxylamino-2,6-dinitrotoluene (4HA26DNT), 2-amino-4,6-dinitrotoluene (2A46DNT), and 4-amino-2,6-dinitrotoluene (4A26DNT) were obtained from AccuStandard, Inc. (New Haven, CT).

Microorganism, media, and culture conditions For inoculum, *E. coli* JM 109 (pGEM4z) was cultured in Luria–Bertani (LB) broth overnight at 37°C and aerated via agitation at 150 rpm. Cells were regrown under the same condition at an inoculum/medium ratio of 1:15 (v/v).

Transformation of TNT Anaerobic TNT transformation assays were performed in an anaerobic chamber filled with anaerobic gas (N_2 85%; H_2 5%; CO_2%) or pure N_2 gas. Aerobically pregrown *E. coli* cells were harvested in the exponential growth phase by centrifugation at 8,110 *g* and 4°C for 10 min at a culture OD_{600} of 1.0. The cell pellets were washed twice with sodium phosphate buffer (PBS, 100 mM, pH 6.5) and resuspended in PBS by adjusting the OD_{600} to the required value. The TNT transformation assay was initiated by adding a small amount of TNT stock solution (100 mM in acetonitrile) to the culture at 30°C and immediate mixing by vortexing. Control experiments were performed by adding TNT to acid-killed cell suspensions (HCl, 1 N). At a defined time after adding TNT, 1-ml aliquots were removed, mixed with 50 μl of 1 N HCl (to stop microbial activity) and 5 μl of 100 mM ascorbate (to minimize autooxidation). Cell pellets were removed by spinning at 11,122 *g* for 5 min. The supernatant was subject to HPLC analysis to detect TNT and transformation products. Details on the analytical techniques have been previously reported (Yin et al. 2004).

Product toxicity measurement To quantify the relationship between the degree of cell inactivation and the amount of TNT transformed, experiments were performed to assess cell activity after 1 cycle of TNT reduction and product removal. In the first cycle, different concentrations of TNT (C_i=0, 30, 140, and 430 μM) were added to 300 μg/ml of cells (OD_{600}=1.0) in the presence of 20 mM glycerol at 30°C. After all the TNT had disappeared in all reactions (24 h), the cells were harvested by centrifuging at 8,110 *g* and 4°C for 10 min. The cell pellets were washed once with sodium phosphate buffer (PBS, 100 mM, pH 6.5) and resuspended in PBS by adjusting the OD_{600} to 1.0. A second cycle of activity was initiated with the recovered cells by adding 400 μM of TNT in the presence of 20 mM glycerol at 30°C. TNT depletion was measured, and initial reaction rates were determined based on zero-order kinetics of TNT consumption or HADNT formation. By comparing the residual activities in the second cycle, the degree of cellular inactivation was calculated. The amount of cellular inactivation was expressed as a decrease in the active biomass protein $\Delta X = X_i\left(1 - \frac{v_i}{v_{i,0}}\right)$, where X_i is the initial cellular protein concentration (in mg/l), while $v_{i,0}$ and v_i are the initial TNT removal or HADNT formation rates (in μM/min) during the second cycle, without or with previous exposure and transformation of a specified amount of TNT, respectively.

Kinetic model development

Reductive TNT transformation is an enzymatic reaction since cell-inactivated controls did not display any TNT depletion (Yin et al. 2004). Because oxygen may interact in a complex fashion with reductive TNT transformation (e.g., it may be a competitive substrate for a TNT reductase which belongs to the respiratory chain, or it may be a physiological sink for reducing power), all the experiments were performed in an anaerobic chamber to avoid oxygen interference. The kinetic model, hence, does not consider oxygen as an interfering substance.

The model considers TNT as the major substrate which is reduced. Intracellular reducing power (RH) is concomitantly oxidized (to R). TNT transformation intermediates are considered to inactivate enzymes (Honeycutt et al. 1996), while TNT itself can display self-inhibition (Park et al. 2002a,b). As a result, the basic Michaelis–Menten (MM) kinetic expression was modified to depict TNT reduction. The basic Michaelis–Menten equation is:

$$\frac{\mathrm{d}[\mathrm{TNT}]}{X\,\mathrm{d}t} = -k_m\left(\frac{[\mathrm{TNT}]}{K_s + [\mathrm{TNT}]}\right), \quad (1)$$

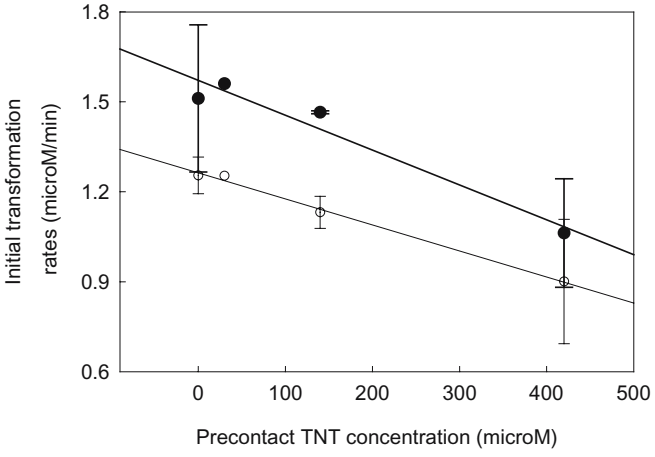

Fig. 1 Product toxicity measured by comparing the initial transformation rates of the same cell concentrations preexposed to different concentrations of TNT (C_i=0, 30, 140, and 430 μM). Two experimental transformation rates are shown: depletion rates of TNT (○) and formation rates of HADNT (●)

where k_m is the maximum rate coefficient (in μmol/mg/min) and K_s is the half-saturation coefficient (in μM) for TNT. [TNT] is the molar TNT concentration (μM), and X is the active cell concentration (measured as cellular protein, mg/l).

Intracellular reducing power (RH) limitation was modeled by inclusion of a second term in the Michaelis–Menten expression, and a stoichiometric link between reducing power consumption and TNT transformation (Segel 1993):

$$\frac{d[TNT]}{dt} = -k_m\left(\frac{[TNT]}{K_s + [TNT]}\right)\left(\frac{[RH]}{K_N + [RH]}\right)X, \tag{2}$$

$$\alpha = \frac{d[RH]}{d[TNT],} \tag{3}$$

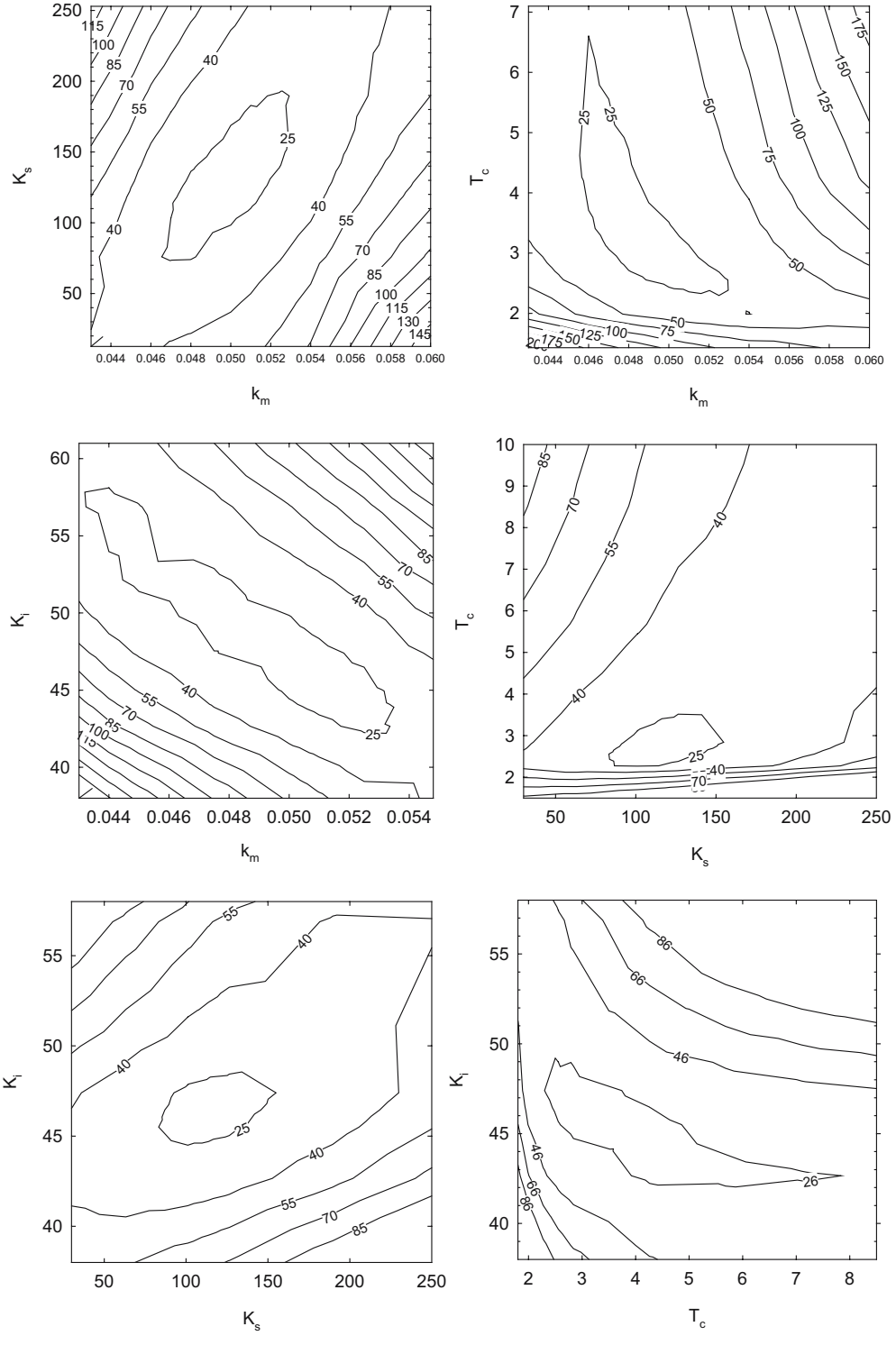

Fig. 2 Contour plots of the parameter estimation response surface for the Michaelis–Menten model incorporating product toxicity and substrate inhibition by fixing any two of the parameters (k_m, K_s, T_c, and K_i) while varying the other two. Best-fit parameter values: k_m=0.05 μmol/mg/min, K_s=126.27 μM, T_c=2.84 μmol/mg cell protein, K_i=47.44 μM

Table 1 Best-fit parameters for Michaelis–Menten-type models and results of *F*-test to evaluate significance of additional parameter inclusion (experimental data are presented in Fig. 3a)

Model parameter and *F*-test	Michaelis–Menten with product toxicity and substrate inhibition	Michaelis–Menten with product toxicity	Michaelis–Menten with substrate inhibition	Michaelis–Menten
k_m (μmol/mg/min)	0.05	0.01	0.09	0.01
K_s (μM)	126.27	0.62	314.14	0.65
T_c (μmol TNT/mg cell protein)	2.84	1.96	–	–
K_i (μM)	47.44	–	21.89	–
WSSD	21.78	97.73	27.44	122.74
F value	16.12	218.85	16.09	
$F_{0.05}$	7.01	7.01	7.01	

where [RH] is an aggregate measure of intracellular reducing power (μM), K_N is the half-saturation coefficient (in μM) for RH, and α is a stoichiometric coefficient (μM RH/μM TNT) indicating the molar amount of reducing power consumed per mole of TNT transformed.

Substrate inhibition was modeled via the Haldane modification of the Michaelis–Menten expression:

$$\frac{d[TNT]}{dt} = -k_m \frac{[TNT]}{K_s + [TNT] + \frac{[TNT]^2}{K_i}} X, \quad (4)$$

where K_i is the substrate inhibition coefficient (in μM) for TNT (Park et al. 2002a,b).

Cell inactivation was described with a linear product toxicity expression:

$$\frac{dX}{dt} = \frac{1}{T_c} \frac{d[TNT]}{dt}, \quad (5)$$

where T_c is the cell transformation capacity (μmol TNT/mg cellular protein), dX is the amount of cell activity reduced (in mg/l) and d[TNT] is the amount of TNT transformed (in μM) (Alvarez-Cohen and McCarty 1991).

The preceding nonlinear ordinary differential equations were solved by a fourth-order Runge–Kutta approximation in an MS office Excel spreadsheet. Parameter estimation was performed by minimization of the sum of squared differences between measured and model data points using both Excel VBA macro programming and Solver optimization routine. The Newton gradient method with forward differences was used, and the parameter estimation routine was started from several different points to ensure that global minima were obtained. When several reduction profiles were fit simultaneously, residuals of individual profiles were weighted by the corresponding initial TNT concentration to ensure similar contributions of all profiles to parameter estimation. *F*-tests were performed to evaluate whether significant model improvement was attained by inclusion of additional model parameters (Beck and Arnold 1977).

Results

Initial experiments revealed that TNT depletion profiles could not be described by simple Michaelis–Menten (MM) kinetics. For example, rates seemed to decrease with reaction progress faster than predicted, while—especially at higher TNT concentrations and lower cellular protein concentrations—incomplete TNT removal was documented.

Three processes were examined as the cause of this non-Michaelis–Menten behavior: reducing power limitation, product toxicity, and substrate inhibition. Our previous results revealed that resting cell transformation of TNT could be significantly enhanced by provision of an external electron donor, probably because it resupplements the internal reducing power, RH, consumed during TNT transformation (Yin et al. 2004). Hence, in subsequent experiments, we either provided an excess of reducing power (in form of glycerol), or explicitly considered RH as a limiting factor.

Product toxicity and substrate inhibition

Product toxicity was evaluated by quantifying residual TNT transformation rates after an initial round of TNT trans-

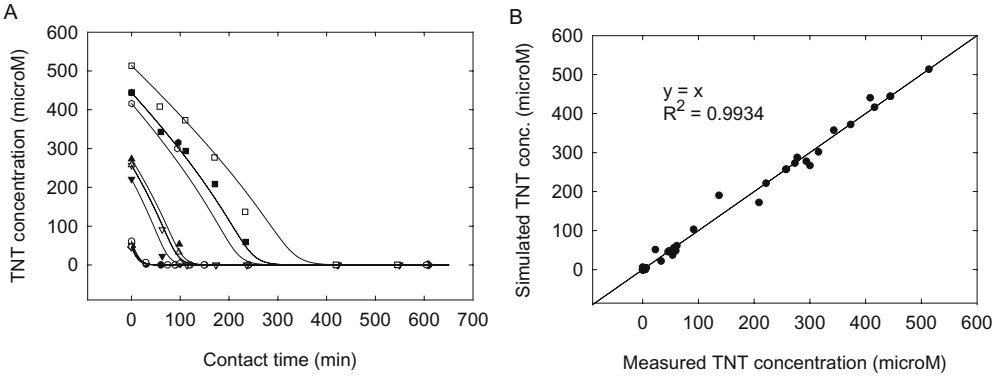

Fig. 3 Best fits of TNT reduction profiles by *E. coli* in the presence of excess glycerol employing a Michaelis–Menten model incorporating product toxicity and substrate inhibition. **a** Experimental and best-fit depletion profiles. **b** Experimental vs best-fit concentrations

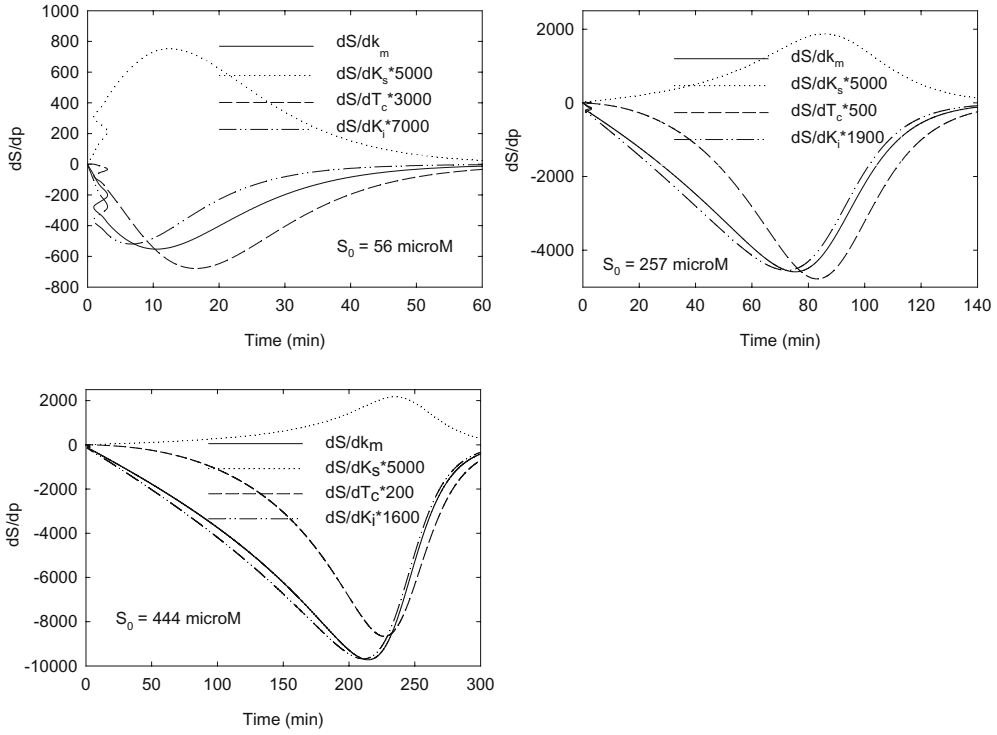

Fig. 4 Sensitivity plots for k_m, K_s, T_c, and K_i in a Michaelis–Menten model incorporating product toxicity and substrate inhibition at three initial TNT concentrations. Assumed parameter values: k_m=0.05 μmol/mg/min, K_s=126.27 μM, T_c=2.84 μmol/mol, K_i=47.44 μM

formation in the presence of excess glycerol (20 mM). Comparing the initial TNT transformation rates of cells preexposed to different concentrations of TNT (C_i=0, 30, 140, and 430 μM) yielded product toxicity, measured as transformation capacity, T_c, of 6.9 μmol TNT/mg total cellular protein. A very similar T_c value (5.2 μmol TNT/mg cellular protein) was measured when the decrease in HADNT formation rates after TNT exposure was considered (Fig. 1).

A biokinetic model incorporating product toxicity and substrate inhibition [Eqs. (4 and 5)] was then considered to describe TNT depletion profiles with excess glycerol, when intracellular reduction power (RH) is a nonlimiting factor.

Kinetic parameter estimation

Parameters were estimated by minimization of the weighted sum of squared differences (WSSD) between measured and model data points (12 profiles, 42 data points). Constraining all parameters to be positive, the optimization routine was started from several different starting points. All runs converged to unique solutions (even when examined parameter ranges were increased multifold, e.g., T_c from 0–50 μM TNT/mg cellular protein), supporting that a global minimum was obtained. Contour plots of response surface near the global minimum are presented by fixing any pair of parameters while varying all others (Fig. 2). Best-fit parameter values clearly altered with the chosen model form, but the inclusion of additional parameters, T_c and K_i, were statistically justified based on *F*-tests (Table 1). Linear regression of the fitted versus experimental TNT profiles for all data sets indicated an excellent model fit across the experimental data sets (Fig. 3).

Parameter identifiability

Sensitivity analyses were performed to test the robustness of the parameter estimation routine as a function of initial substrate and cellular protein concentrations. Because TNT concentration was the measured response in this study, the following sensitivity equations were analyzed: $dS/dk_m=f_1(t)$, $dS/dK_s=f_2(t)$, $dS/dT_c=f_3(t)$, $dS/dK_i=f_4(t)$, where t is the contact time. The first derivative of S versus t with respect to k_m, K_s, T_c, and K_i were determined by a numerical algorithm employing a fourth-order Runge–Kutta integration method. The resulting sensitivity plots were appro-

Table 2 Results of Monte Carlo simulations to evaluate the identifiability of parameters as affected by experimental measurement error

Parameter	k_m	K_s	T_c	K_I
True value	0.050	126.273	2.840	47.436
S_0=400 μM				
Mean	0.050	126.036	2.862	47.304
Standard deviation	0.004	2.715	0.339	3.505
Coefficient of variance	0.077	0.022	0.118	0.074
S_0=50 μM				
Mean	0.050	126.204	2.906	47.287
Standard deviation	0.001	0.527	1.138	2.890
Coefficient of variance	0.022	0.004	0.392	0.061

priately scaled to determine the degree of superimposition on one another.

The sensitivity profiles for the four parameters (k_m, K_s, T_c, and K_i) were well separated at low initial TNT concentration (56 μM), while the separation became poorer at higher initial TNT concentrations (257 and 440 μM) (Fig. 4). There was some correlation between k_m and K_i at TNT concentration of 440 μM, but the two sensitivity curves were still separable suggesting that the parameters were identifiable under this condition. Quantitatively, k_m has the highest impact on TNT depletion in all plots (by at least 2 orders of magnitude). In summary, the sensitivity analysis suggests that unique estimates of all four parameters (k_m, K_s, T_c, and K_i) can be obtained from batch experiments within the range of initial TNT concentrations that were experimentally employed.

Monte Carlo simulations were subsequently performed to determine the robustness and accuracy of the parameter estimation routine considering typical measurement error. The standardized difference between the measured TNT profile and the best-fit profile was set equal to the standardized error for each measurement. These standardized errors followed a normal distribution (normality test: p=0.751, mean −0.037, standard deviation 0.102). Uncorrelated, random, normally distributed errors with a zero mean and calculated standard deviation were subsequently added to the simulated TNT profiles created with the Michaelis–Menten plus toxicity and inhibition model (MM+T_c+K_i). One hundred realizations of two ensembles, each containing random measurement error, were created and biokinetic parameters (k_m, K_s, T_c, and K_i) were estimated from each of those realizations. One ensemble was based on estimated parameters for TNT profiles at an initial concentration of 50 μM, and the other ensemble was based on an initial concentration of 400 μM. Monte Carlo simulations indicated that the parameter estimation routine retrieved best-fit parameters very close to the true values (Table 2), with acceptable coefficients of variance for the four parameters (k_m, K_s, T_c, and K_i) (2.2–7.7%) with the lowest precision for T_c (11.8–39.2%). Hence, typical measurement errors will not significantly deteriorate parameter estimation at any TNT concentration; although the estimated T_c has much more variability at a low TNT concentration (50 μM). Despite its relatively high variability, the 95% confidence interval for T_c lies in the range of 2.42–3.39 (data not shown), which is still close to the true estimated value 2.84 μM. Overall, the results indicate that, on average, the parameter estimation method can obtain accurate parameter estimates, although replicate profiles may be necessary to overcome variability in the measurements.

Reducing power limitation

With product toxicity and substrate inhibition identified and quantified, TNT transformation by *E. coli* resting cells was examined without excess glycerol to evaluate the effect of reducing power limitation. Experiments were conducted at an initial TNT concentration ranging from 0 to 300 μM and constant cellular protein concentration (300 mg

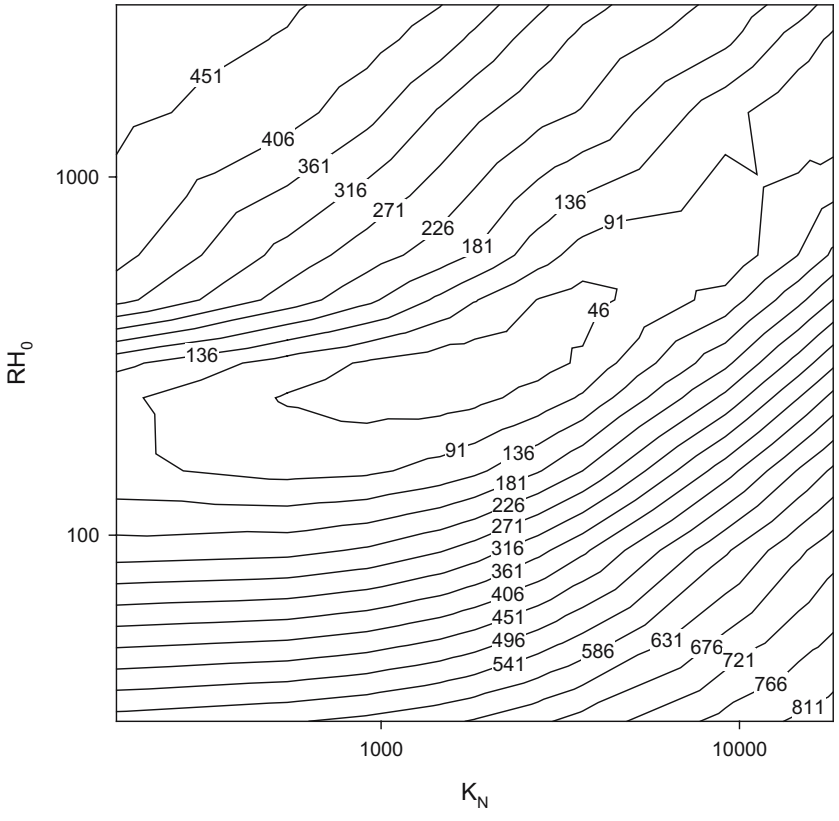

Fig. 5 Contour plots of the parameter estimation response surface for K_N and RH_0 in the Michaelis–Menten model incorporating product toxicity, substrate inhibition, and reducing power limitation with k_m, K_s, T_c, and K_i fixed at 0.05 μmol/mg/min, 126.27 μM, 2.84 μmol/mg cellular protein, and 47.44 μM respectively

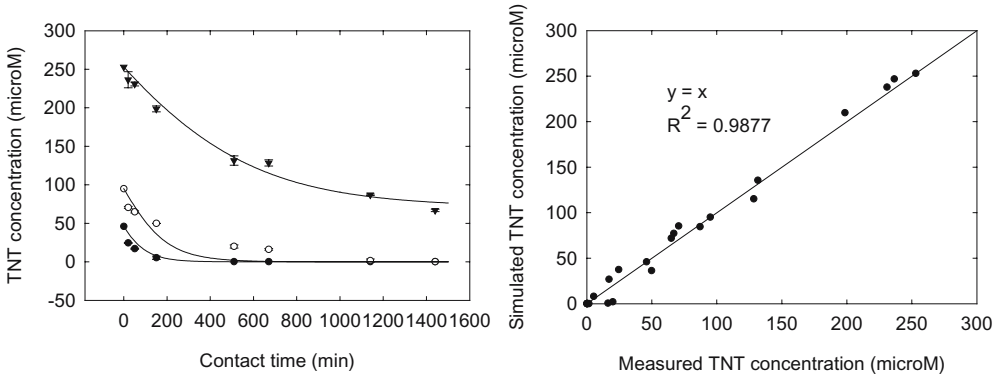

Fig. 6 Best fits of TNT reduction profiles by resting cells of *E. coli* employing a Michaelis–Menten model incorporating product toxicity, substrate inhibition and reducing power limitation. **a** Experimental and best-fit depletion profiles. **b** Experimental vs best-fit concentrations

protein/l). The modified Michaelis–Menten model, incorporating product toxicity and substrate inhibition, yielded poor fits to the TNT depletion profiles, suggesting the need to explicitly consider reducing power. As a result, Eqs. (2 and 3) were applied to incorporate the limitation of reducing power. Retaining the four parameters, k_m, K_s, T_c, and K_i, at the same values as identified in the excess glycerol case, K_N and α are the only parameters that required estimation. The parameter α measures the molar ratio of RH oxidized to TNT reduced (d[RH]/d[TNT]). In our observation, TNT was reduced to HADNTs in a first step, theoretically accompanied with two electrons transfer per TNT molecule transformed (Yin et al. 2004). However, a molar ratio of 1.66 was chosen, because our earlier experimental work revealed an incomplete molar recovery of HADNT isomers from TNT (Riefler and Smets 2002). There is no direct and clear way to measure the intracellular reducing power concentration (RH) as it is unknown, to date, what fraction of the total intracellular reducing power equivalents contributes electrons to TNT reduction. As a result, RH_0 was a parameter to be estimated. Starting from different initial estimates of RH_0 and K_N, a global solution converged on best-fit estimates for RH_0 and K_N of 302 and 1,825 μM, respectively (three profiles, 24 data points) (Fig. 5). Linear regression of fitted versus experimental TNT concentrations indicated a good model fit (Fig. 6). These results demonstrate the necessity of incorporating intracellular reducing power limitation to depict TNT transformation kinetics in resting cells of *E. coli*.

Table 3 Literature reported nitroreductase activities and extrapolated whole-cell unit based activities

Enzymes/whole cells	Electron acceptor (s)	Reductase activity (nmol/min/mg of protein)	
		Pure enzyme	Whole cells
NAD(P)H:flavin mononucleotide oxidoreductase (Riefler and Smets 2002)	TNT	319,000	2,300[a]
NfsA (Zenno et al. 1996b)	4-Nitrotoluene	1,000	7.2[a]
NfsB (Zenno et al. 1996a)	4-Nitrotoluene	400	2.88[a]
E. coli whole cells (this study)	TNT	NA	50

[a]Extrapolated assuming that the specific enzyme constitutes 7.2‰ of total cellular protein

Discussion

TNT reductive transformations have been extensively documented in various microbes and plants (Esteve-Núñez et al. 2001; Spain 1995). For example, with the *E. coli* strain used in this report, TNT is sequentially transformed to 4HA26DNT and 2HA46DNT (with 4HA26DNT as the major isomer), followed by formation of 24D(HA)6NT and ADNT isomers (4A26DNT, with sporadic detection of 2A46DNT), all of which—except 24D(HA)6NT—were detected in the presence of residual TNT, indicating concomitant reduction, with 24DA6NT as the most reduced transformation product detected (Yin et al. 2004). However, reports on comprehensive modeling of TNT reduction have been sparse. TNT transformation has only been described by pseudo-first, second-order, or simple Michaelis–Menten kinetics thus far (Wang et al. 2003; Watrous et al. 2003). A detailed Michaelis–Menten-based model has been reported with respect to the reduction of TNT by a pure enzyme, NAD(P)H:flavin mononucleotide oxidoreductase (Riefler and Smets 2002). In this study, whole-cell transformation of TNT by *E. coli* was thoroughly investigated and modeled with a modified Michaelis–Menten kinetic model. Half-saturation coefficient (K_s) in whole cells was estimated at 126.27 μM, whereas for the pure enzyme NAD(P)H:flavin mononucleotide oxidoreductase, this value was 187 μM. The similar affinity expressed in these K_s values suggests that mass transfer across the cell membrane does not severely limit the reaction.

Nitroreductases NfsA and/or NfsB have been implicated in catalyzing TNT reduction by *E. coli* (Yin et al. 2004). Reported specific nitroreductase activities were compared to our whole-cell observations by using a typical nitroreductase yield (7.2‰ of total cellular protein; Zenno et al. 1996a,b) (Table 3). Our estimated TNT reductase activity of 50 nmol/min/mg of total cellular protein falls within the

range of the above known nitroreductase activities (between 2.88 and 2,300 nmol min/mg of total cellular protein). Compared with the activities of NfsA and NfsB toward 4-nitrotoluene (Zenno et al. 1996a,b), our estimate was about eightfold higher, which would be consistent with the thermodynamically favored reduction of TNT per its one-electron reduction potential (Riefler and Smets 2002).

Product toxicity was estimated at 5.2 μmol TNT/mg of total cellular protein, equivalent to ~700 μmol/mg of NfsA (Zenno et al. 1996a,b) assuming the same protein fraction as above, and on the same scale as the measured toxicity of 398 μmol TNT/mg of enzyme for the NAD(P)H:FMN oxidoreductase (Riefler and Smets 2002). Further, our analysis clearly supported the need to include a product toxicity term to permit adequate simulation of the TNT depletion profiles (Table 1).

Resting cells of *E. coli* consume their own reducing power for TNT transformation through cometabolism, and we provided a simple approach to account for changes in the intracellular reducing power in the model. However, as the relevant initial intracellular reducing power (RH_0), to date, can not be analytically defined and tracked, it was treated as a parameter and subject to best parameter estimation. The best-fit RH_0 value of 302 μM was, satisfactorily, consistent with experimentally measured intracellular concentrations of NADH under aerobic conditions (de Graef et al. 1999; Riefler and Smets 2002), while the half-saturation coefficient K_N (1,825 μM) was in a range consistent with reports for examined pure enzymes (Riefler and Smets 2002). The depletion profiles of intracellular reducing power (RH) were based on the assumed stoichiometric linear relationship with TNT consumption (Riefler and Smets 2002). While a reasonable stoichiometric coefficient was obtained from reports on a similar enzyme, experimental confirmation of this parameter value and its constancy are necessary (Riefler and Smets 2002). Clearly, a more rigorous assessment of the physical correctness of the proposed model and parameters will be contingent on a direct identification and quantification of *E. coli*'s intracellular reducing power that drives TNT reduction and the experimental confirmation of this stoichiometric relationship.

This study presents the first comprehensive model of whole-cell level TNT reductive transformation in *Escherichia coli*, and provides new insight into the mechanism of microbial TNT reduction. Here we demonstrate that TNT bioreduction profiles can be described by Michaelis–Menten kinetics incorporating three factors: product toxicity, substrate inhibition, and reducing power limitation. The presented kinetic model successfully describes our experimental data at various initial TNT concentrations under reducing power excess or limited scenarios; and can form the basis for further examinations in TNT bioreduction (e.g., examination of involved enzymes, identification of internal reducing power pools).

Acknowledgements This work was supported by an award from the National Science Foundation to BFS and TKW (BES-0114126). We thank Yingge Qu for helping us with Excel VBA macro programming and Cairn Ely for editorial assistance. The experiments comply with current U.S. laws covering the conditions in which they were performed.

Reference

Adrian NR, Arnett CM, Hickey RF (2003) Stimulating the anaerobic biodegradation of explosives by the addition of hydrogen or electron donors that produce hydrogen. Water Res 37:3499–3507

Alvarez-Cohen L, McCarty PL (1991) A cometabolic biotransformation model for halogenated aliphatic compounds exhibiting product toxicity. Environ Sci Technol 25:1381–1387

Beck JV, Arnold KJ (1977) Parameter estimation in engineering and science. Wiley, New York, NY

Criddle CS (1993) The kinetics of cometabolism. Biotechnol Bioeng 41:1048–1056

Daun G, Lenke H, Knackmub H-J, Reub M (1999a) Experimental investigations and kinetic and models for the cometabolic biological reduction of trinitrotoluene. Chem Eng Technol 21:308–313

Daun G, Lenke H, Knackmuss HJ, Reuss M (1999b) Experimental investigations and kinetic models for the cometabolic biological reduction of trinitrotoluene [Reprint]. Chem Eng Technol 22:308–313

de Graef MR, Alexeeva S, Snoep JL, Teixeira de Mattos MJ (1999) The steady-state internal redox state (NADH/NAD) reflects the external redox state and is correlated with catabolic adaptation in *Escherichia coli*. J Bacteriol 181:2351–2357

Dodard SG, Renoux AY, Powlowski J, Sunahara GI (2003) Lethal and subchronic effects of 2,4,6-trinitrotoluene (TNT) on *Enchytraeus albidus* in spiked artificial soil. Ecotoxicol Environ Saf 54:131–138

Esteve-Núñez A, Caballero A, Ramos JL (2001) Biological degradation of 2,4,6-trinitrotoluene. Microbiol Mol Biol Rev 65:335–352

Fiorella P, Spain J (1997) Transformation of 2,4,6-trinitrotoluene by *Pseudomonas pseudoalcaligenes* JS52. Appl Environ Microbiol 63:2007–2015

Fuller ME, Manning JF Jr (1997) Aerobic gram-positive and gram-negative bacteria exhibit differential sensitivity to and transformation of 2,4,6-trinitrotoluene (TNT). Curr Microbiol 35:77–83

Gibbs MD, Nevalainen KMH, Bergquist PL (2001) Degenerate oligonucleotide gene shuffling (DOGS): a method for enhancing the frequency of recombination with family shuffling. Gene 271:13–20

Homma-Takeda S, Hiraku Y, Ohkuma Y, Oikawa S, Murata M, Ogawa K, Iwamuro T, Li S, Sun GF, Kumagai Y, Shimojo N, Kawanishi S (2002) 2,4,6-Trinitrotoluene-induced reproductive toxicity via oxidative DNA damage by its metabolite. Free Radic Res 36:555–566

Honeycutt ME, Jarvis AS, McFarland VA (1996) Cytotoxicity and mutagenicity of 2,4,6-trinitrotoluene and its metabolites. Ecotoxicol Environ Saf 35:282–287

Huang S, Lindahl PA, Wang C, Bennett GN, Rudolph FB, Hughes JB (2000) 2,4,6-Trinitrotoluene reduction by carbon monoxide dehydrogenase from *Clostridium thermoaceticum*. Appl Environ Microbiol 66:1474–1478

Kurinenko BM, Yakovleva GY, Denivarova NA, Abreimova YV (2003) Specific toxic effects of 2,4,6-trinitrotoluene on *Bacillus subtilis* SK1. Appl Biochem Microbiol 39:275–278

Labidi M, Ahmad D, Halasz A, Hawari J (2001) Biotransformation and partial mineralization of the explosive 2,4,6-trinitrotoluene (TNT) by rhizobia. Can J Microbiol 47:559–566

Lewis T, Goszczynski S, Crawford R, Korus R, Admassu W (1996) Products of anaerobic 2,4,6-trinitrotoluene (TNT) transformation by *Clostridium bifermentans*. Appl Environ Microbiol 62:4669–4674

McCormick NG, Feeherry FE, Levinson HS (1976) Microbial transformation of 2,4,6-trinitrotoluene and other nitroaromatic compounds. Appl Environ Microbiol 31:949–958

Oh BT, Shea PJ, Drijber RA, Vasilyeva GK, Sarath G (2003) TNT biotransformation and detoxification by a *Pseudomonas Aeruginosa* strain. Biodegradation 14:309–319

Park C, Kim T-H, Kim S, Lee J, Kim S-W (2002a) Biokinetic parameter estimation for degradation of 2,4,6-trinitrotoluene (TNT) with *Pseudomonas putida* KP-T201. J Biosci Bioeng 94:57–61

Park C, Kim T, Kim S, Kim S, Lee J (2002b) Enhanced biodegradation of 2,4,6-trinitrotoluene (TNT) with various supplemental energy sources. J Microbiol Biotechnol 12:695–698

Preuss A, Rieger PG (1995) Biodegradation of nitroaromatic compounds. Plenum Press, New York

Riefler RG, Smets BF (2002) NAD(P)H:flavin mononucleotide oxidoreductase inactivation during 2,4,6-trinitrotoluene reduction. Appl Environ Microbiol 68:1690–1696

Sax NI, Lewis RJ (1987) Hawley's condensed chemical dictionary, 11th edn. Van Nostrand, New York

Segel IH (1993) Enzyme kinetics: behavior and analysis of rapid equilibrium and steady-state systems. Wiley, New York, NY

Spain JC (1995) Biodegradation of nitroaromatic compounds. Annu Rev Microbiol 49:523–555

van Beelen P, Burris DR (1995) Reduction of the explosive 2,4,6-trinitrotoluene by enzymes from aquatic sediments. Environ Toxicol Chem 14:2115–2123

Wang C, Lyon DY, Hughes JB, Bennett GN (2003) Role of hydroxylamine intermediates in the phytotransformation of 2,4,6-trinitrotoluene by *Myriophyllum aquaticum*. Environ Sci Technol 37:3595–3600

Watrous MM, Clark S, Kutty R, Huang S, Rudolph FB, Hughes JB, Bennett GN (2003) 2,4,6-Trinitrotoluene reduction by an Fe-only hydrogenase in *Clostridium acetobutylicum*. Appl Environ Microbiol 69:1542–1547

Yin H, Wood TK, Smets BF (2004) Reductive transformation of TNT by *Escherichia coli*: pathway description. Appl Microbiol Biotechnol. Published online: 13 October 2004

Zenno S, Koike H, Tanokura M, Saigo K (1996a) Gene cloning, purification, and characterization of NfsB, a minor oxygen-insensitive nitroreductase from *Escherichia coli*, similar in biochemical properties to FRase I, the major flavin reductase in *Vibrio fischeri*. J Biochem (Tokyo) 120:736–744

Zenno S, Koike H, Kumar A, Jayaraman R, Tanokura M, Saigo K (1996b) Biochemical characterization of NfsA, the *Escherichia coli* major nitroreductase exhibiting a high amino acid sequence homology to Frp, a *Vibrio harveyi* flavin oxidoreductase. J Bacteriol 178:4508–4514

Zenno S, Kobori T, Tanokura M, Saigo K (1998) Conversion of NfsA, the major *Escherichia coli* nitroreductase, to a flavin reductase with an activity similar to that of Frp, a flavin reductase in *Vibrio harveyi*, by a single amino acid substitution. J Bacteriol 180:422–425